Durability of Biodegradable Polymers for the Conservation of Cultural Heritage

Maria C. Mistretta[1], Francesco P. La Mantia[1]*, Vincenzo Titone[1], Bartolomeo Megna[1], Luigi Botta[1] and Marco Morreale[2]

[1] Department of Engineering, University of Palermo, Palermo, Italy, [2] Faculty of Engineering and Architecture, Kore University of Enna, Enna, Italy

The use of polymers for conservation of cultural heritage is related to the possibility to slow down or stop natural deterioration which, in many cases, corresponds to stopping the entrance of liquid water and to favor spontaneous water vapor removal. Unfortunately, hydrophobicity is generally favored by surface roughness and thus competitive with transparency. It is therefore important to find an optimal balance hydrophobicity, transparency and durability (especially to photooxidation). However, polymers typically used for applications in this field come from non-renewable resources and are not biodegradable. In this work, the mechanical, structural, and optical properties of PLA, PBAT, and a PBAT/PLA blends, as well as surface properties and water vapor permeability, were investigated before and after exposure to UV irradiation, in order to evaluate their durability and suitability for conservation of cultural heritage.

Keywords: biodegradable polymers, durability, cultural heritage, conservation, mechanical properties, permeability

INTRODUCTION

The most important characteristics of polymers for conservation of cultural heritage are related to the capability to slow down, or possibly stopping, the ongoing deterioration; however, since one mostly causes of deterioration are related to the presence of water, the most important goal is to stop the entrance of liquid water and to facilitate spontaneous water vapor removal. Therefore, hydrophobicity is particularly important. However, one of the surface properties most affecting the actual hydrophobicity is the roughness: typically, hydrophobicity increases on increasing the surface roughness. Since the latter is competitive with transparency (which typically decreases on increasing the roughness), a further challenge is to tailor the polymer coating thickness in order to find the best compromise in terms of hydrophobicity, transparency, and durability. Furthermore, a good durability requires a suitable resistance to photooxidation and a good water vapor permeability after treatment.

The first category of polymeric materials to be actually investigated for application in this field was represented by acrylic polymers (Feller, 1978, 1994; Favaro et al., 2006). Their actual resistance to water and photooxidation was evaluated (Melo et al., 1999; Borgia et al., 2001; Chiantore and Lazzari, 2001) finding an unsatisfactory stability under UV irradiation, as well as inadequate water barrier properties over time. Thus, fluorinated polymers were taken into account as possible alternatives, showing some encouraging results, but also questionable surface adhesion properties (Frediani et al., 1982; Torrisi, 2008; Licchelli et al., 2013). Therefore, further efforts were focused

on copolymers or blends from both acrylic and fluorinated polymers (Mazzola et al., 2003; Malshe and Sangaj, 2009). Furthermore, silanes and siloxanes (Tsakalof et al., 2007; Vacchiano et al., 2008; Ershad-Langroudi et al., 2017) also showed interesting properties in terms of impermeability and protection against color loss, although these were strongly dependent on the specific substrate. Polymers from cellulose have been extensively used and studied for application on cultural heritage, finding that both cellulose ethers (Feller and Wilt, 1990) and nitrate (Selwitz, 1988) have some stability issues. Finally, PEG was recently proposed in order to consolidate collapsible soil, highlighting interesting properties (Zimbardo et al., 2019).

However, all of the above discussed solutions are based on traditional polymers, coming from non-renewable resources and not biodegradable, with the well-known related issues of environmental impacts: the increasing demand for better use of natural resources and reduction of the environmental impacts related to the use of plastics currently require the search for alternative and more environment-friendly solutions (Bastioli, 2005; Song et al., 2009; Lo Re et al., 2013; Morreale et al., 2015). Furthermore, one of the main problems related to the use for conservation of cultural heritage (especially, for stone conservation) is related to reversibility (Andreotti et al., 2018). In fact, any protective coating should be removable in the future if needed, or at least retreatable. Unfortunately, traditional organic coatings have been found to be hardly removable (even using solvents) after some years of exposure to outdoor conditions, and go on aging and progressively losing their properties. This suggests, therefore, the use of biodegradable materials in replacement for non-biodegradable one; in particular, biodegradable polymers should spontaneously disappear from the underlying stone, after their properties (namely, water barrier and repellence properties) are lost (Andreotti et al., 2018).

With regard to the actual suitability of biodegradable polymers for cultural heritage conservation, the Literature does not report a high amount of data in this context.

Ocak et al. (2009) studied the behavior of some biodegradable polymers such as zein, chitosan, polyhydroxybutyrate (PHB), and poly-lactic acid (PLA) in terms of protection capability of marble surfaces under SO_2. They found that the latter two were less suitable to protect against sulphatation.

Giuntoli et al. (2012) prepared some PLA samples, functionalized through fluorinated alcohols as co-initiators of polymerization, finding that the polymers coming from the L-lactide showed higher water protection in comparison to those coming from a racemic mixture of L- and D-lactide.

Ocak et al. (2015) investigated the behavior of a PLA-montmorillonite nanocomposite in terms of protection of marble surfaces against air pollution. The presence of the nanofiller evidenced an increased hydrophobicity, and therefore higher impermeability to environment waters and, at the same time, reduced water vapor permeability.

Sacchi et al. (2012) performed several investigations on different systems such as a lactic acid omopolymer and two lactic acid copolymers (copolymerized with a commercial low molecular weight perfluoropolyether). Their suitability to protect marble against aging (simulated by thermohygrometric cycles and UV irradiation) was studied, finding an enhancement of the water-repellent behavior in comparison to non-fluorinated PLA; this was kept even after thermohygrometric aging, while UV aging led, in some cases, to a detachment between the polymer layer and the marble substrate, depending on the kind of marble examined.

Andreotti et al. (2018) studied the behavior of PHA for stone protection, finding interesting results in terms of effectiveness and compatibility, while further improvements of durability and applicability still seem necessary.
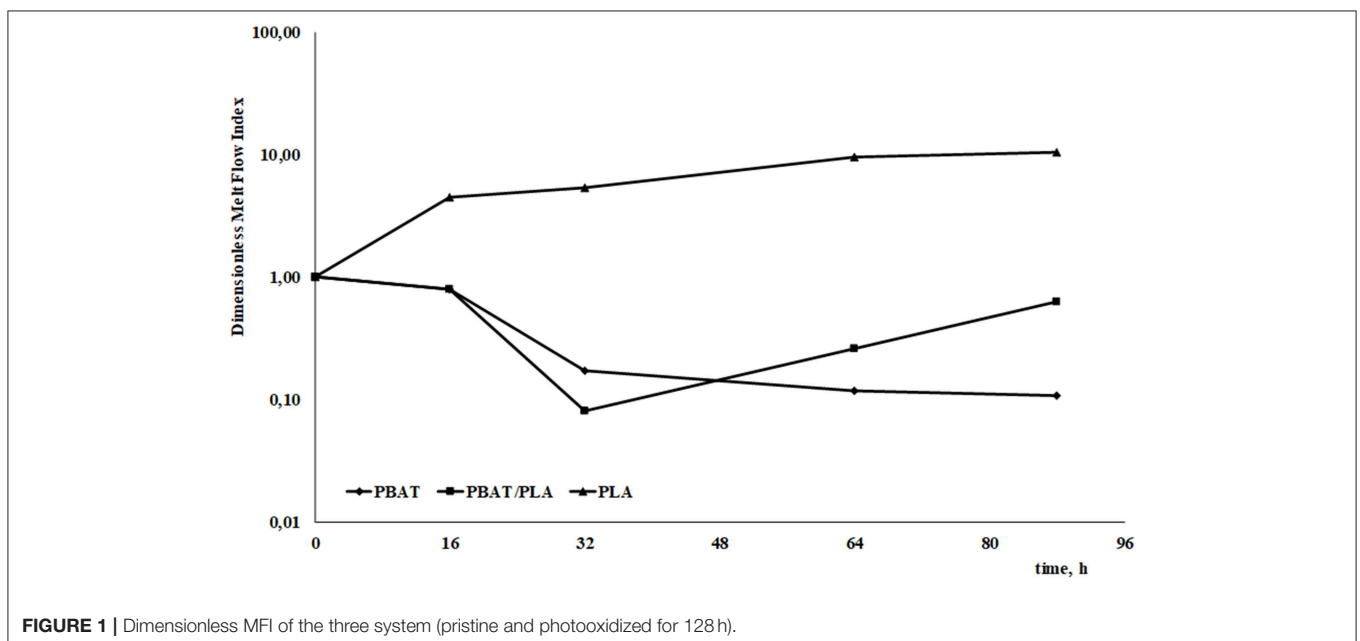

FIGURE 1 | Dimensionless MFI of the three system (pristine and photooxidized for 128 h).

Xing et al. (2017) prepared PBAT/lignin UV-blocking films. More in details, they grafted bio-based 10-undecenoic and oleic acids on soda lignin via solvent methods and then blended the lignin, as well as the lignin ester derivatives, with PBAT. They found good lignin dispersion, thermal stability and retaining of tensile properties up to 10–20 wt% filler loading, and very good UV-barrier properties even after 50 h of irradiation.

It can be deduced from this brief literature report, that the suitability of a polymer system as protective layer on stone is dependent on its durability, which in its turn is related to the loss of hydrophobicity. The latter can depend on photooxidation (photooxidation, in fact, leads to the increase of polar groups on the surface, and therefore to an increase of hydrophilicity). Furthermore, most of the available information regards PLA, while less information is available about other polymers, such as for instance PBAT.

The photooxidation behaviors of PLA and PBAT have been reported in the literature (Ikada, 1997; Tsuji et al., 2006; Janorkar et al., 2007; Nakayama and Hayashi, 2007; Kijchavengkul et al., 2010; Zaidi et al., 2010; Gardette et al., 2011; Stloukal et al., 2012). With regard to PLA, the mechanisms involved are a photolytic mechanism leading to the breaking of the C-O bond in the macromolecular chain and a photooxidative mechanism leading to the formation of hydroperoxides and, in turn, of carboxylic acids and ketones (Janorkar et al., 2007); moreover, also the Norrish II mechanism can be involved (Tsuji et al., 2006; Nakayama and Hayashi, 2007), although under UV irradiation at wavelengths higher than 300 nm, different chain scission mechanisms were found (Gardette et al., 2011). With concern to the PBAT, degradation can occur via Norrish I and II chain scission, and can also lead to significant crosslinking phenomena due to the free radicals generated during the Norrish I path (Kijchavengkul et al., 2010; Stloukal et al., 2012).

In this work, therefore, we focused on the investigation on the mechanical and optical properties of PLA, PBAT, and a PBAT/PLA blend, with particular concern on the behavior after exposure to UV irradiation. The main objective was to evaluate the suitability and durability of these materials for conservation of cultural heritage.

EXPERIMENTAL

The materials used in this work were: a PLA sample, commercially known as Ingeo 4032D (NatureWorks, USA), having a MFI equal to 7 g/10 min (at 210°C and 2.16 kg), a density of 1.24 g/cm^3 and a melting point between 155 and 170°C; a PBAT sample, commercially known as Ecoflex (BASF, Germany) with a MFI between 2.7 and 4.9 g/10 min; a sample of PBAT/PLA blend, commercially known as Ecovio (BASF, Germany) with a MFI between 5 and 11 g/10 min. The neat, non-aged systems were compared also to a reference commercial fluoropolymer sample, Fluoline HY (CTS, Italy), that is a high molecular weight fluorinated elastomer, typically used as protective layer for porous stone substrates.

Sheets of all the samples (previously conditioned in a vacuum oven at 70°C for 4 h) were prepared by compression molding at $T = 170°C$ (except for the PLA which was molded at 190°C) in a Carver (USA) laboratory press.

The obtained specimens (thickness of about 300 μm) were exposed to accelerated weathering in a "Q-UV" chamber (Q-Labs Corp., USA) containing eight "UVB-313" lamps up to about 128 h, according to the procedures described elsewhere (Morreale et al., 2013) at 70°C.

Mechanical (tensile) tests were carried out according to ASTM D638 both on weathered and unweathered specimens (90 × 10 × 0.3–0.5 mm) using an Instron (USA) mod. 3365 universal testing machine. The elastic modulus was measured at 1 mm/min deformation speed. When the deformation reached 10%, the crosshead speed was increased to 100 mm/min until final breaking. The values of the elastic modulus, E, tensile strength, TS, and elongation at break, EB, were calculated as average of 10 tests, with an adequate reproducibility (±7%).

FTIR spectra in ATR mode were obtained by using a Perkin-Elmer (USA) Spectrum One spectrometer, using the embedded SpectrumOne software. The spectra were obtained through 16 scans with a 4 cm^{-1} resolution. Measurements were obtained from the average of triplicate samples. Particular attention was focused on the carbonyl peak centered at 1,720 cm^{-1}, which was used to measure the dimensionless carbonyl index (ratio between the carbonyl peak area of the sample at a given photooxidation time and carbonyl peak area of the unirradiated sample) in order monitoring the photooxidation.

UV-Vis spectra were obtained on triplicates using a Specord 252 (Analytik Jena, Germany) spectrometer in the 190–1,100 nm range.

Melt Flow index (MFI) values were measured using a CEAST (Italy) equipment at 170°C under a 2.16 kg load, as the average of four measurements (data reproducibility: ±5%).

The cross-linked fraction was evaluated by measuring the residual gel fraction obtained after Soxhlet extraction using boiling tetrahydrofuran (THF) on triplicates.

Enthalpy of fusion of the samples was measured by differential scanning calorimetry (DSC), using a Shimadzu (Japan) DSC-60 apparatus, with 5°C/min heating rate from 40 to 200°C, as the average of four measurements (data reproducibility: ±6%).

TABLE 1 | Enthalpy of fusion of pristine (unirradiated) and photooxidized (128 h) samples.

	Exposure time, h	ΔH(PLA), J/g	ΔH(PBAT), J/g
PLA	0	1.59 ± 0.06	—
PLA	128	48.41 ± 1.9	—
PBAT	0	—	5.45 ± 0.27
PBAT	128	—	5.57 ± 0.28
PLA/PBAT	0	1.22 ± 0.07	4.28 ± 0.26
PLA/PBAT	128	1.62 ± 0.1	0.56 ± 0.03

For the blend sample, the enthalpies of fusion of the two phases are reported.

Contact angle measurements (in order evaluating wettability of the investigated materials) were performed using a First Ten Angstrom (USA) FTA1000C system, with demineralized water (on four samples, data reproducibility: ±4%).

Water vapor permeability measurements were performed on samples (diameter 4.5 cm) coming from the above mentioned compression-molded sheets, at 25°C and 50% relative humidity, using a BYK-Gardner (Germany) permeability cup. Permeability constant was calculated as the average of four measurements by normalizing the measured weight loss of each sample against the sample thickness (data reproducibility: ±7%), according to the procedures described elsewhere (Iizuka et al., 2016; Hendrickx et al., 2017).

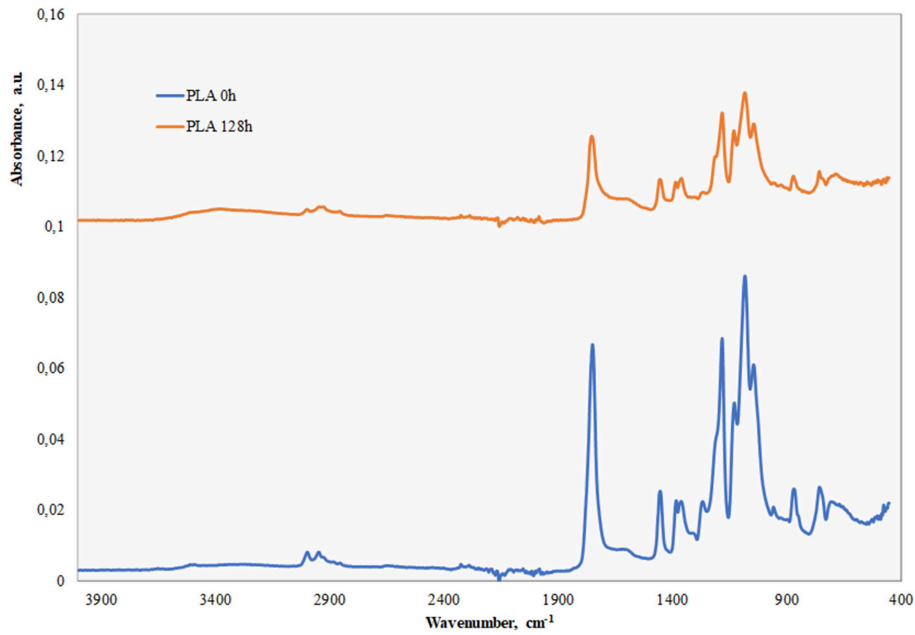**FIGURE 2 |** ATR spectra of pristine and photooxidized PLA.
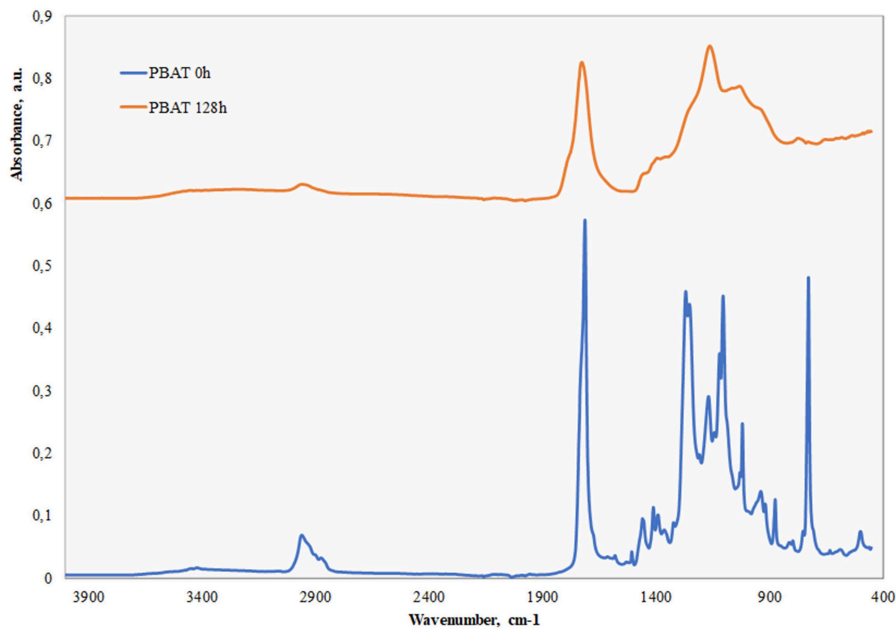

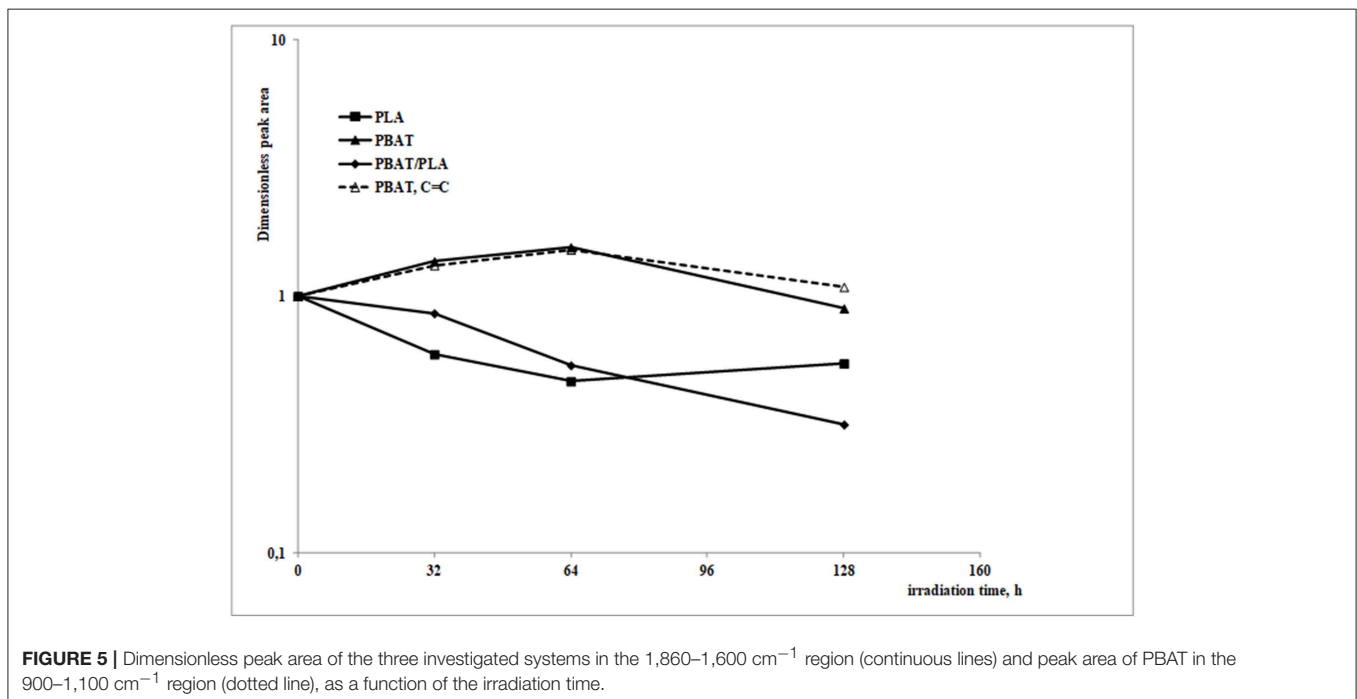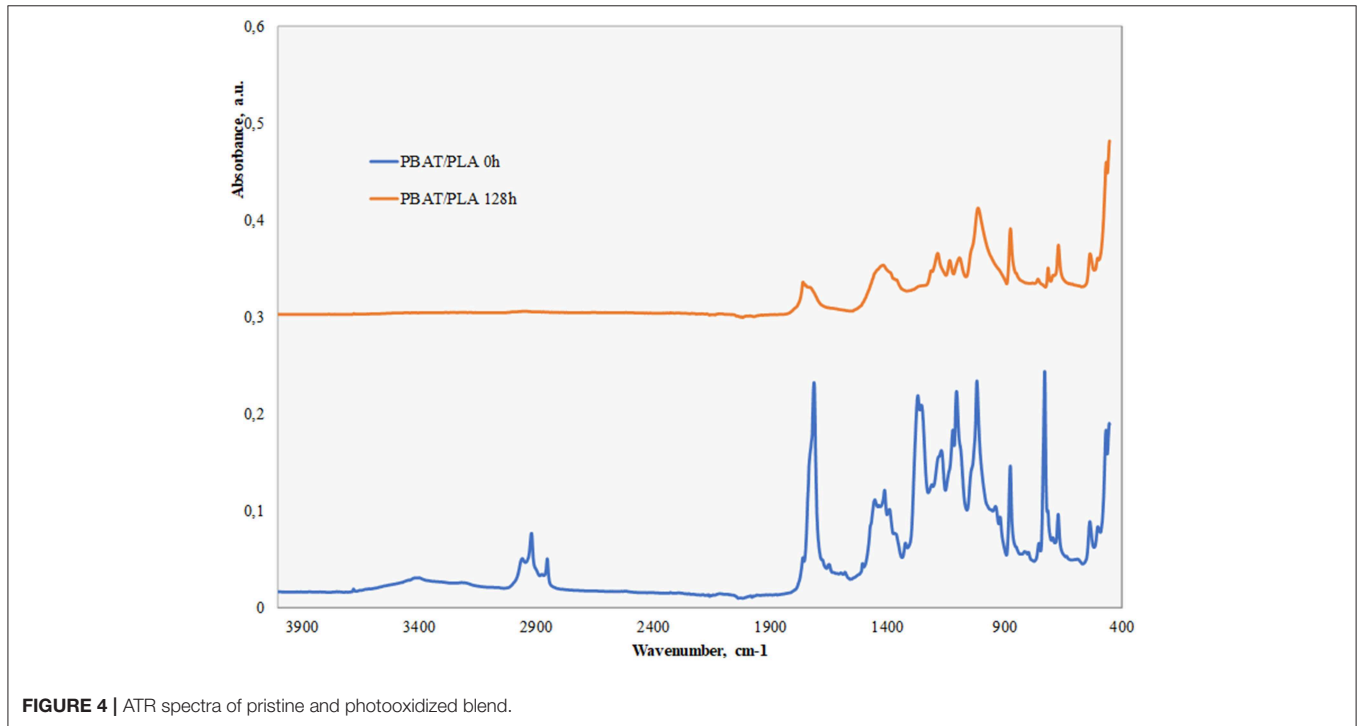**FIGURE 3 |** ATR spectra of pristine and photooxidized PBAT.

RESULTS AND DISCUSSION

In **Figure 1**, the dimensionless MFI values are reported, as a function of the irradiation time.

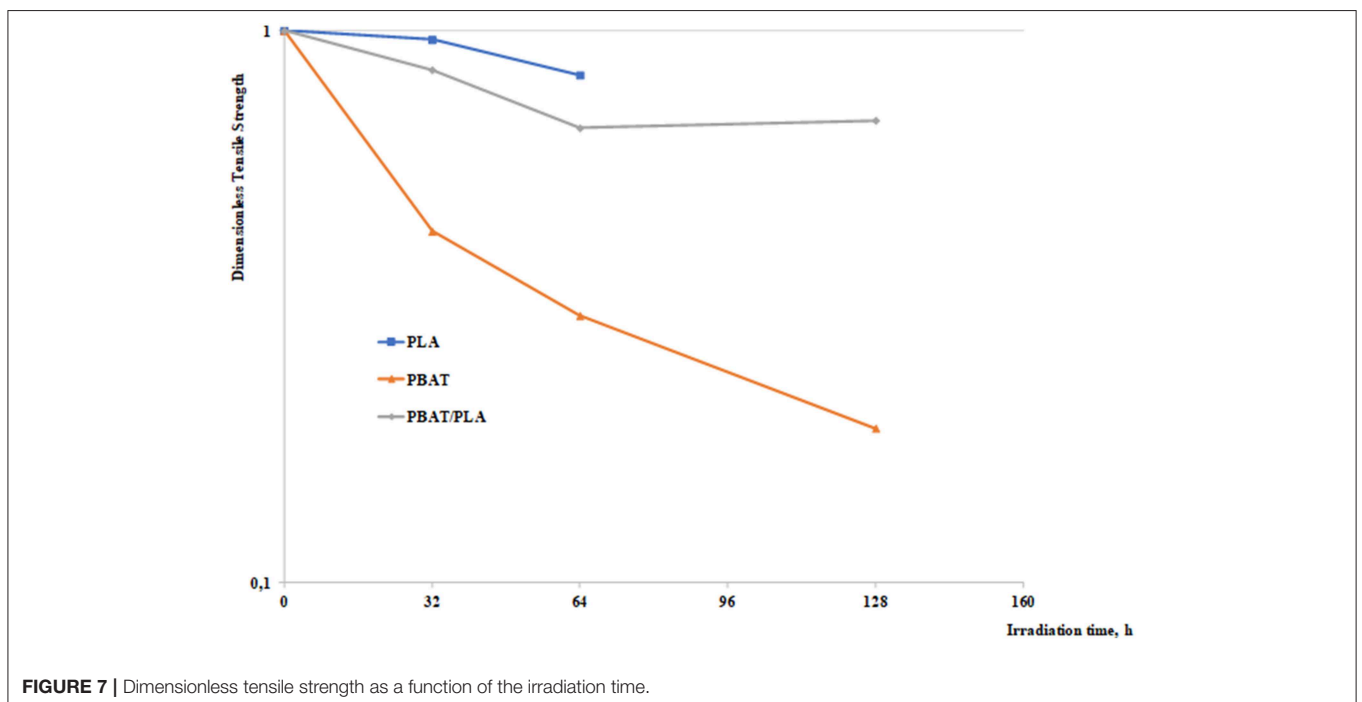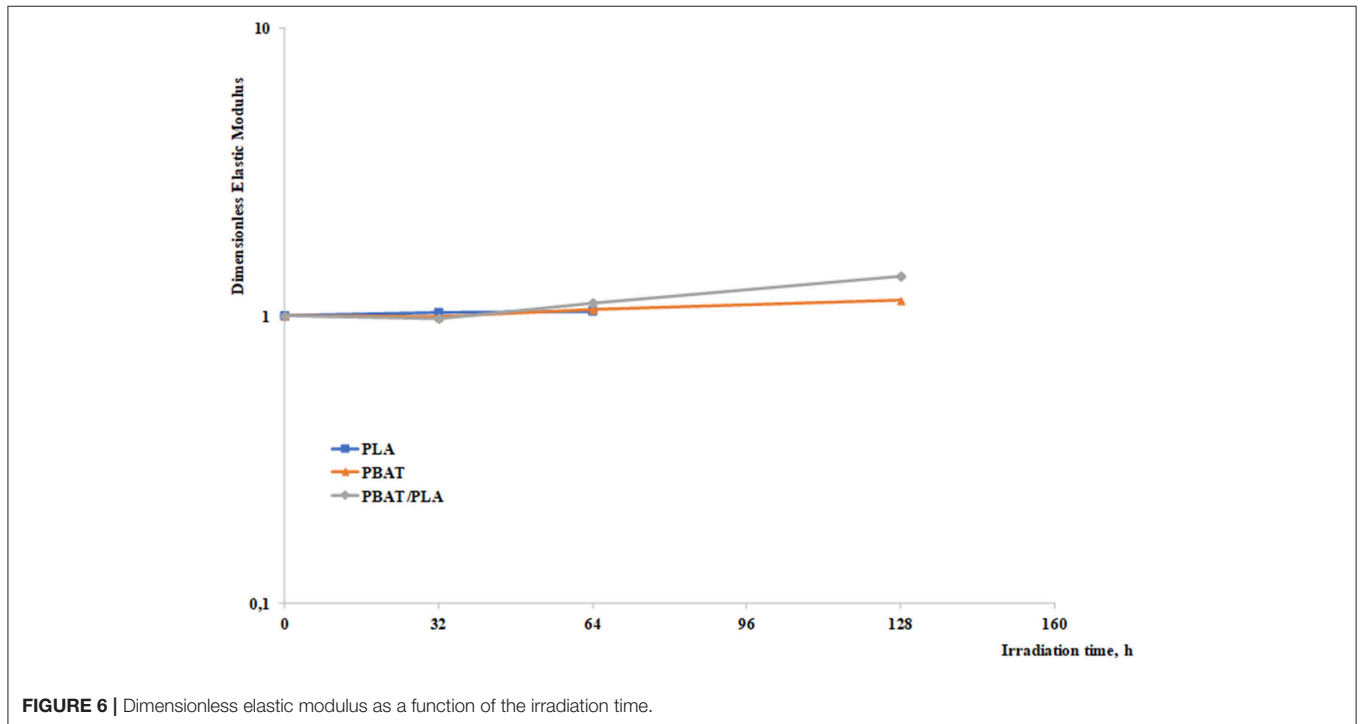The gel fraction values of the three pristine (unirradiated) samples were obviously zero; after 128 h irradiation they were found to be still zero in the PLA sample, while they increased to 6.8 in the PBAT, and 22.6 in the PLA/PBAT.

The photooxidation of PLA, therefore, gives rise to a decrease of the molecular weight—increase of the MFI value—and no presence of cross-linking was detected. These results indicate that the photooxidation proceeds to breakage of the macromolecules

FIGURE 4 | ATR spectra of pristine and photooxidized blend.

FIGURE 5 | Dimensionless peak area of the three investigated systems in the 1,860–1,600 cm^{-1} region (continuous lines) and peak area of PBAT in the 900–1,100 cm^{-1} region (dotted line), as a function of the irradiation time.

and oxidation of the carbon atoms. PBAT and the PBAT/PLA blend show similar behaviors, with a decrease of molecular weight but, on the contrary, a formation of cross-linking structures is observed in both of the systems. According to the reported results, it is evident that the cross-linking occurs only in the PBAT phase and that the increase of the crosslinking in the blend, in comparison to neat PBAT, suggests that PLA degradation (which follows a chain scission path) and the related degradation products promote PBAT degradation (which, on the other hand, mainly follows a crosslinking path). The observation of **Figure 1** further indicates that the PBAT undergoes significant crosslinking phenomena (in particular, after 32 h) resulting in a

FIGURE 6 | Dimensionless elastic modulus as a function of the irradiation time.

FIGURE 7 | Dimensionless tensile strength as a function of the irradiation time.

decrease of the MFI, and this is even more important in the blend, where the crosslinking of the PBAT fraction is able to lead to a decrease of the MFI even though the greater part of the blend is composed by PLA. On the other hand, the role of the chain-scission degradation of PLA gains importance on increasing the photooxidation time, leading to a gradual reversal of the trend.

The enthalpies of fusion of the three samples, virgin and photooxidized, are reported in **Table 1**.

It can be observed that, in substantial agreement with the crosslinking (gel fraction) data, the crystallinity generally decreases on increasing the crosslinking rate.

Figures 2–4 report the ATR spectra of virgin and photooxidized PLA, PBAT, and PLA/PBAT blend, respectively.

As regards the PLA, the main peaks to be observed are: 871 cm^{-1} (-CH- bending), 1,453 (-CH3 bending), 1,745 cm^{-1} (C=O axial deformation vibration), 1,087, 1,129, and 1,184 cm^{-1} (stretching of the –CO- bond).

In the case of PBAT, the main peaks are: 729 cm^{-1} (-CH2- stretching), 1,104, 1,120, and 1,165 cm^{-1} (-CO- stretching), and 1,730 cm^{-1} (C=O axial deformation vibration). The blend shows the typical peaks from both of the two components, in particular at 1,745, 1,730, 1,453, 1,087–1,104–1,165, 871, and 729 cm^{-1}. The reported peaks are in agreement with literature data (Dias Fernandes et al., 2017).

The ATR spectra of the PLA show a decrease of the peak located at 1,745 cm^{-1}, thus indicating a reduction of the esters, but at the same time the overall carbonyl peak area does not change significantly, thus suggesting chain scission degradation, in agreement with the hypotheses derived from the previously discussed data. With regard to PBAT, a somewhat similar decrease and a widening of the carbonyl peak was observed, but in this case also two shoulders at 1,790 and 1,750 cm^{-1} appear, related to the formation of free carbonyls and low molecular weight esters, respectively. These two findings suggest that Norrish-I type chain scission reactions occurred (Gardette et al., 2011).

Furthermore, a broadened peak around 1,000 cm^{-1} was observed, indicating the formation of C=C bonds, thus suggesting that also Norrish-II type chain scission reactions occurred (Gardette et al., 2011).

With regard to the blend, the peak modifications substantially mirror those of the individual components. However, such peak modifications are significantly sharper.

In order to deepen the analysis, the dimensionless carbonyl peak area (calculated as the ratio between the peak from 1,600 to 1,860 cm^{-1} at a given photooxidation time and the same before photooxidation) as a function of irradiation time is reported in **Figure 5**.

As previously discussed, a reduction of the carbonyl peak upon increasing the UV exposure time should happen, mainly attributable to chain scission reactions (especially Norrish I type). However, as the oxidation goes on, it gives rise to different oxidation species such as free carbonyls and low molecular

TABLE 2 | Elastic modulus, tensile strength and elongation at break of the three unirradiated samples.

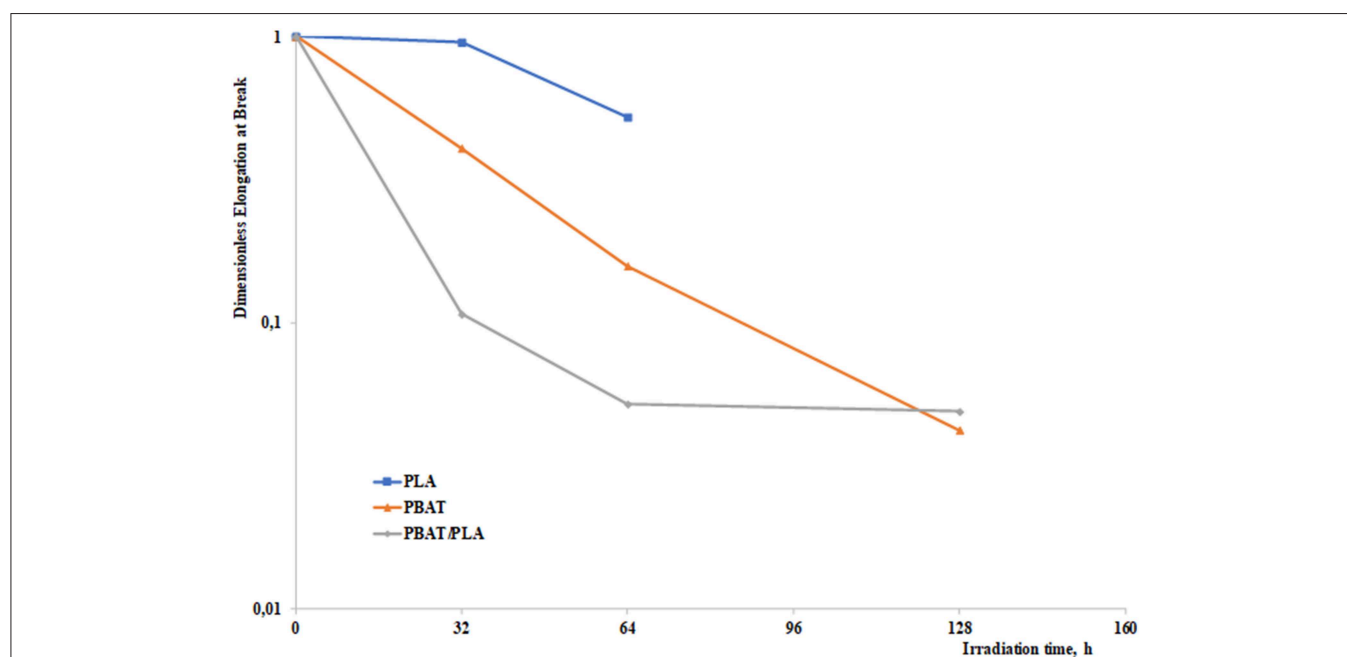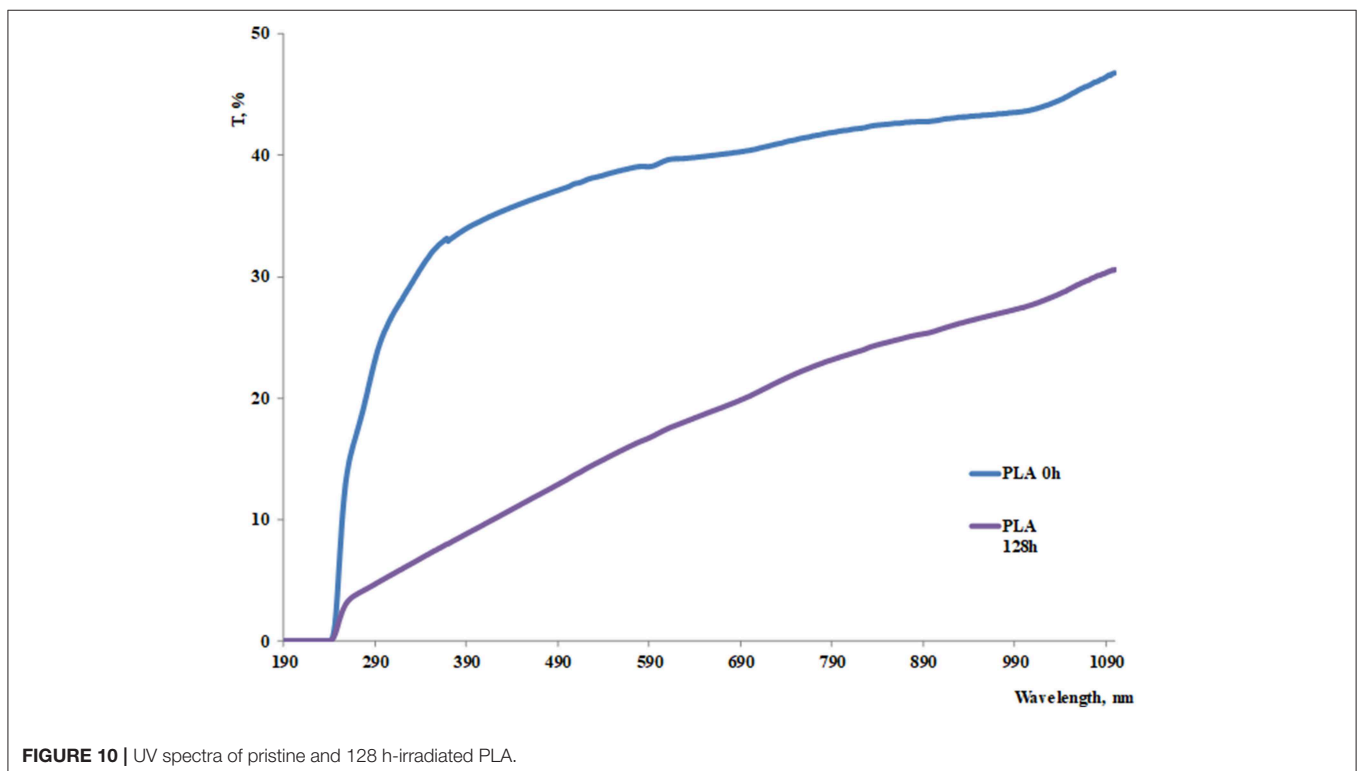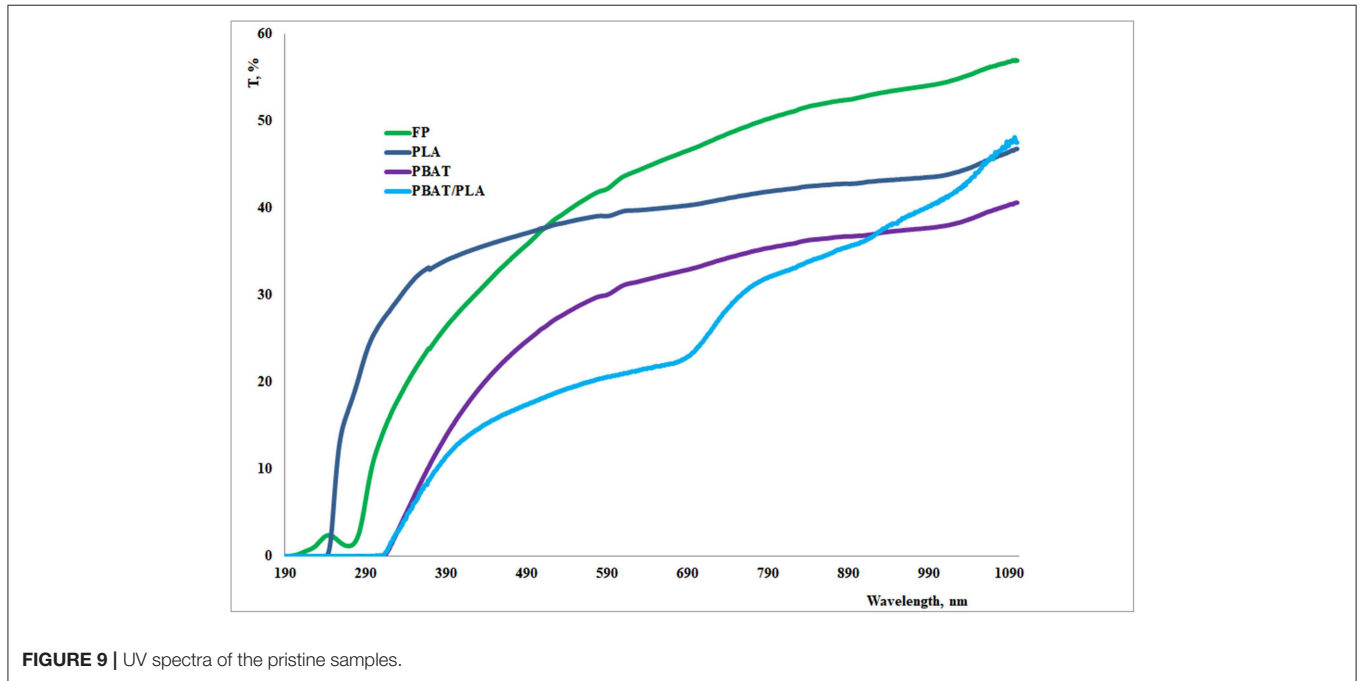|	E, MPa	TS, MPa	EB, %
PLA	1585 ± 63	42 ± 1.7	4 ± 0.2
PBAT	48 ± 3.4	20 ± 1.4	820 ± 41
PLA/PBAT	111 ± 7.8	9.3 ± 0.5	327 ± 20

FIGURE 8 | Dimensionless elongation at break as a function of the irradiation time.

weight esters, which allow the overall carbonyl peak area to not decrease much, or to keep practically constant; in the case of PBAT, C=C bonds are formed, reasonably due to Norrish II type chain scission reactions, which slightly increase the related peak area (between 900 and 1,100 cm^{-1}, see dotted line in the same **Figure 5**).

The degradation has a deep effect on the mechanical properties that can strongly change during the photooxidation. In **Figures 6–8**, the dimensionless values of the elastic modulus, E, tensile strength, TS, and elongation at break, EB, are drawn as a function of the irradiation time for the three materials (PLA values reported only up to 64 h, since

FIGURE 9 | UV spectra of the pristine samples.

FIGURE 10 | UV spectra of pristine and 128 h-irradiated PLA.

the samples became excessively brittle after that exposure time). The dimensionless values have been calculated by dividing the values at each irradiation time by those of the same virgin (unirradiated) polymer, which are reported in **Table 2**.

As expected, the blend has intermediate properties in terms of rigidity and deformability, while the tensile strength experiences antagonistic effects.

It can be observed that the photooxidation had significantly detrimental effects on the ductility (EB) of the materials, in
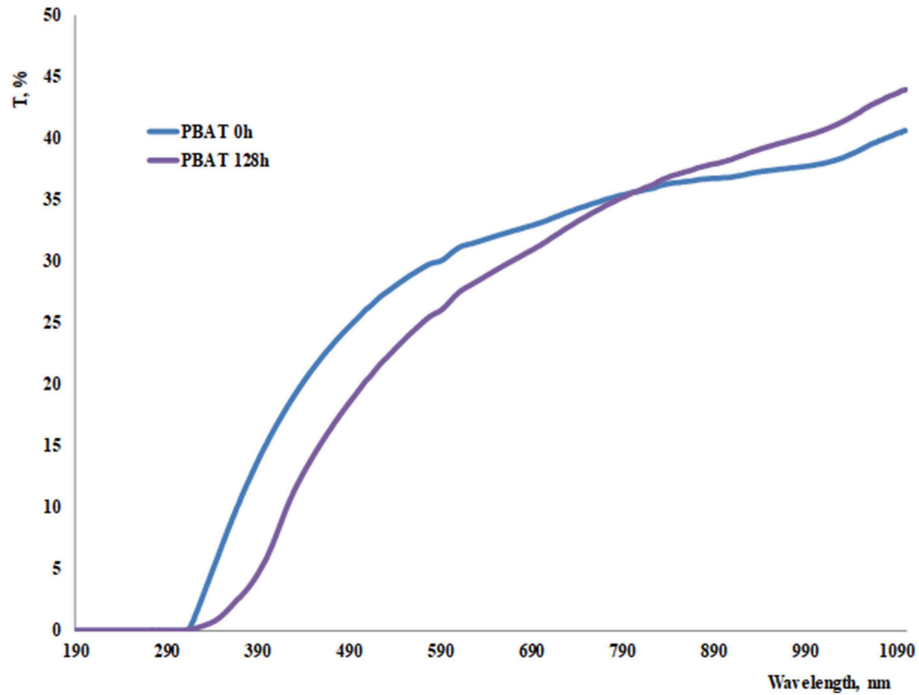

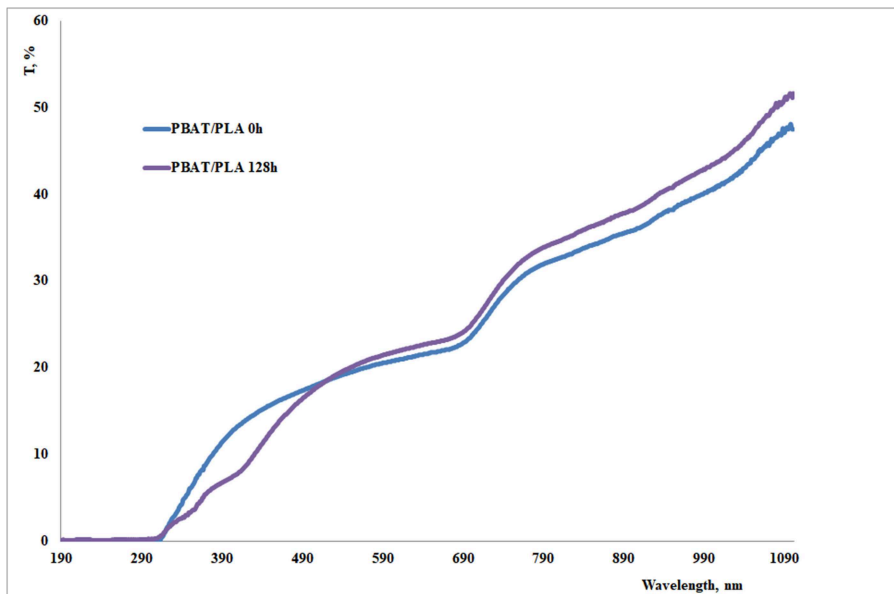**FIGURE 11 |** UV spectra of pristine and 128 h-irradiated PBAT.

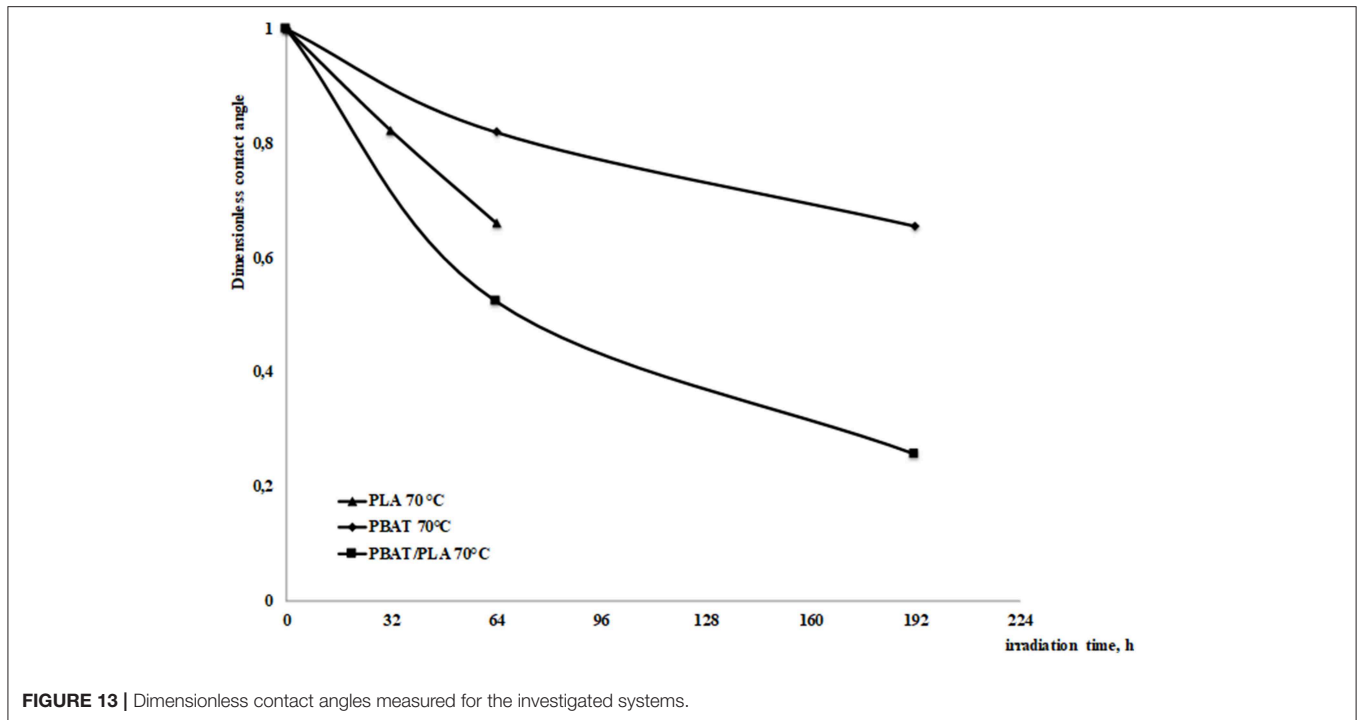**FIGURE 12 |** UV spectra of pristine and 128h-irradiated PBAT/PLA blend.

FIGURE 13 | Dimensionless contact angles measured for the investigated systems.

agreement with the previous discussions on the reduction of molecular weight and crosslinking phenomena. With regard to the tensile resistance (TS), all of the three materials undergo (as expectable on the basis of the above consideration) a reduction, but with remarkable differences: while the PLA undergoes limited worsening of the TS, the PBAT undergoes a drop. This may be due to the different embrittlement kinetics of the two materials (see **Figure 8**), which lead to premature breaking of PBAT. On the other hand, the blend shows a different behavior, with significantly lower reduction of the TS in comparison to the PBAT, in apparent contrast with the deductions that could be drawn on the basis of the embrittlement. This is explainable, however, considering that the blend experienced increased crosslinking phenomena, which mitigate the loss of tensile resistance. At the same time, there is some increase or no change of the modulus, due to the above discussed phenomena of crosslinking and chain scission.

Due to its use for covering cultural heritage, the optical properties play a very important role.

Figure 9 shows the UV spectra of virgin fluoropolymer, PLA, PBAT, and PBAT/PLA blend, while **Figures 10–12** report the comparison to the spectra obtained after 128 h photooxidation of the same samples. The transmittance (and thus transparency) in the visible range (380–740 nm) of the reference fluoropolymer is, on average, slightly higher, however the values of the biodegradable polymers appear to be comparable. On increasing the photooxidation time, it slightly decreases in the PBAT, while the reduction is higher in the PLA; however, in the case of the blend, in the 490–780 nm range, the values are almost unchanged. This suggests that the investigated polymer

blend should be suitable for cultural heritage applications, in terms of maintaining the main optical properties over time, although the use of suitable antioxidants would obviously improve the behavior.

Contact angle measurements at different photooxidation times were measured, and are shown in **Figure 13**.

It was not possible to measure the values of the PLA samples irradiated more than 64 h since the specimens were significantly damaged due to the photooxidation. It is observed that the contact angle decreases on increasing the photooxidation time, due to the increasing amount of polar groups formed during the degradation (as discussed previously) and the increasing rugosity of the surfaces. This is a further confirmation of the interpretations provide with regard to the results coming from spectral analysis.

Finally, the measured values of specific water vapor permeability were found to be 1.35 ± 0.07 g/mm in the reference fluorinated elastomer; with regard to the biodegradable systems, it was found to change from 5.41 ± 0.32 to 2.95 ± 0.37 g/mm in the case of PBAT, and from 6.79 ± 0.47 to 2.88 ± 0.2 g/mm in the case of the PBAT/PLA blend. Therefore, the biodegradable systems are in the same order of magnitude and thus comparable to the reference fluoropolymer. Also in this case, it was not possible to measure the values of the PLA samples irradiated more than 64 h since the specimens were significantly damaged due to the photooxidation It is thus observed that, after the UV aging treatment, the specific permeability significantly decreases in comparison to the neat unirradiated systems. This is in agreement with the previously discussed results, since it can be explained on the basis of the increased crosslinked fraction and the variations of crystallinity degree.

CONCLUSIONS

In this work, the mechanical, structural and optical properties of PLA, PBAT, and a PBAT/PLA blends, as well as surface properties and water vapor permeability, were investigated before and after exposure to UV irradiation. The main objective was to evaluate the suitability and durability of these materials for conservation of cultural heritage.

Photooxidation followed a complex path, involving mainly chain scission in the PLA and crosslinking in the PBAT, while synergistic effects were found in the blend.

The mechanical properties of the blend were intermediate between those of the neat PLA and PBAT; however, the UV exposure led to different worsening of the three systems, pointing out that the blend undergoes more limited decay of the main mechanical properties, in comparison to the neat PBAT.

Water vapor permeability was found to decrease on increasing the exposure time; the UV transmittance in the visible range slightly decreased in the PBAT, while the reduction was higher in the PLA; in the case of the blend, the values in the 490–780 nm range were almost unchanged, although the overall transmittance was lower.

The obtained results suggest that the PBAT/PLA blend investigated in this work could be suitable for cultural heritage applications, and that the next advisable steps should consist in experimenting the addition of suitable antioxidants in order to improve the overall performance.

DATA AVAILABILITY

The datasets generated for this study are available on request to the corresponding author.

AUTHOR CONTRIBUTIONS

FL and MCM designed the experiments. VT, MCM, and LB performed the experiments. All of the authors analyzed the data. FL supervised the work. FL, MM, and BM wrote the paper (original draft, reviewing, and editing).

FUNDING

REFERENCES

Andreotti, S., Franzoni, E., Degli Esposti, M., and Fabbri, P. (2018). Poly(hydroxyalkanoate)s-based hydrophobic coatings for the protection of stone in cultural heritage. *Materials* 11, 1–26. doi: 10.3390/ma11010165

Bastioli, C. (ed). (2005). *Handbook of Biodegradable Polymers*. Akron, OH: iSmithers Rapra Publishing.

Borgia, G. C., Bortolotti, V., Camaiti, M., Cerri, F., Fantazzini, P., and Piacenti, F. (2001). Performance evolution of hydrophobic treatments for stone conservation investigated by MRI. *Magn. Reson. Imaging* 19, 513–516. doi: 10.1016/S0730-725X(01)00281-8

Chiantore, O., and Lazzari, M. (2001). Photo-oxidative stability of paraloid acrylic protective polymers. *Polymer* 42, 17–27. doi: 10.1016/S0032-3861(00)00327-X

Dias Fernandes, T. M., Amorim Moreira Leite, M. C., Furtado de Sousa, A. M., Russi Guimaraes Furtado, C., Alves Escocio, V., and Nazareth de Silva, A. L. (2017). Improvement in toughness of polylactide/Poly(butylene adipate-co-terephthalate) blend by adding nitrile rubber. *Polym. Bull.* 74, 1713–1726. doi: 10.1007/s00289-016-1798-9

Ershad-Langroudi, A., Fadaii, H., and Ahmadi, K. (2017). Silane/siloxane surface treatment for cohesion ability and strengthening agent of historical stone. *Conserv. Sci. J.* 1, 23–31. doi: 10.30699/ics.journal.01.23

Favaro, M., Mendichi, R., Ossola, F., Russo, U., Simon, S., Tomasin, P., et al. (2006). Evaluation of polymers for conservation treatments of outdoor exposed stone monuments, Part I: photo-oxidative weathering. *Polym. Degrad. Stab.* 91, 3083–3096. doi: 10.1016/j.polymdegradstab.2006.08.012

Feller, R. L. (1978). "Standards in the evaluation of thermoplastic resins," in *Proceedings ICOM Committee for Conservation, 5th Triennial Meeting* (Zagreb).

Feller, R. L. (1994). *Accelerated Aging - Photochemical and Thermal Aspects*. Ann Arbor, MI: The J. Paul Getty Trust.

Feller, R. L., and Wilt, M. (1990). *Evaluation of Cellulose Ethers for Conservation*. Getty Conservation Institute. ISBN 0-89236-099-2.

Frediani, P., Manganelli Del Fa', C., Matteoli, U., and Tiano, P. (1982). Use of perfluoropolyethers as water repellents: study of their behaviour on pietra serena a Florentine building stone. *Stud. Conserv.* 27, 31–37. doi: 10.1179/sic.1982.27.1.31

Gardette, M., Therias, S., Gardette, J. L., Murariu, M., and Dubois, P. (2011). Photooxidation of polylactide/calcium sulphate composites. *Polym. Degrad. Stab.* 96, 616–623. doi: 10.1016/j.polymdegradstab.2010.12.023

Giuntoli, G., Rosi, L., Frediani, M., Sacchi, B., and Frediani, P. (2012). FluoroFunctionalized PLA polymers as potential water-repellent coating materials for protection of stone. *J. Appl. Polym. Sci.* 125, 3125–3133. doi: 10.1002/app.36469

Hendrickx, R., Ferreira, E. S., Boon, J. J., Desmarais, G., Derome, D., Angelova, L., et al. (2017). Distribution of moisture in reconstructed oil paintings on canvas during absorption and drying: a neutron radiography and NMR study. *Stud. Conserv.* 62, 393–409. doi: 10.1080/00393630.2016.1181899

Iizuka, S., Murata, K., Sekine, M., and Sato, C. (2016). A novel cup with a pressure-adjusting mechanism for high-temperature water vapor transmission rate measurements. *Polym. Test.* 50, 73–78. doi: 10.1016/j.polymertesting.2015.11.018

Ikada, E. (1997). Photo and biodegradable polyesters. photodegradation behaviors of aliphatic polyesters. *J. Photopolym. Sci. Technol.* 10, 265–270. doi: 10.2494/photopolymer.10.265

Janorkar, A. V., Metters, A. T., and Hirt, D. E. (2007). Degradation of Poly(L-Lactide) films under ultraviolet-induced photografting and sterilization conditions. *J. Appl. Polym. Sci.* 106:1042. doi: 10.1002/app.24692

Kijchavengkul, T., Auras, R., Rubino, M., Alvarado, E., Montero, J. R. C., and Rosales, J. M. (2010). Atmospheric and soil degradation of aliphatic aromatic polyester films. *Polym. Degrad. Stab.* 95, 99–107. doi: 10.1016/j.polymdegradstab.2009.11.048

Licchelli, M., Malagodia, M., Weththimunia, L. M. L., and Zanchia, C. (2013). Waterrepellent properties of fluoroelastomers on a very porous stone: effect of the application procedure. *Prog. Org. Coat.* 76, 495–503. doi: 10.1016/j.porgcoat.2012.11.005

Lo Re, G., Morreale, M., Scaffaro, R., and La Mantia, F. P. (2013). Biodegradation paths of Mater-Bi®/kenaf biodegradable composites. *J. Appl. Polym. Sci.* 129, 3198–3208. doi: 10.1002/app.39027

Malshe, V. C., and Sangaj, N. S. (2009). Fluorinated acrylic copolymers Part I: study of clear coatings. *Prog. Org. Coat.* 53, 207–211. doi: 10.1016/j.porgcoat.2005.03.003

Mazzola, M., Frediani, P., Bracci, S., and Salvini, A. (2003). New strategies for the synthesis of partially fluorinated acrylic polymers as possible materials for the protection of stone monuments. *Eur. Polym. J.* 39, 1995–2003. doi: 10.1016/S0014-3057(03)00110-1

Melo, M. J., Bracci, S., Camaiti, M., Chiantore, O., and Piacenti, F. (1999). Photodegradation of acrylic resins used in the conservation of stone. *Polym. Degrad. Stab.* 66, 23–30. doi: 10.1016/S0141-3910(99)00048-8

Morreale, M., Dintcheva, N. T., and La Mantia, F. P. (2013). Accelerated weathering of PP based nanocomposites: Effect of the presence of maleic anhydryde grafted polypropylene. *eXPRESS Polym. Lett.* 7, 703–715. doi: 10.3144/expresspolymlett.2013.67

Morreale, M., Liga, A., Mistretta, M. C., Ascione, L., and Mantia, F. P. (2015). Mechanical, thermomechanical and reprocessing behavior of green composites from biodegradable polymer and wood flour. *Materials* 8, 7536–7548. doi: 10.3390/ma8115406

Nakayama, N., and Hayashi, T. (2007). Preparation and characterization of poly(L-lactic acid)/TiO2 nanoparticle nanocomposite films with high transparency and effcient photodegradability. *Polym. Degrad. Stab.* 92, 1255–1264. doi: 10.1016/j.polymdegradstab.2007.03.026

Ocak, Y., Sofuoglu, A., Tihminlioglu, F., and Böke, H. (2009). Protection of marble surfaces by using biodegradable polymers as coating agent. *Prog. Org. Coat.* 66, 213–220. doi: 10.1016/j.porgcoat.2009.07.007

Ocak, Y., Sofuoglu, A., Tihminlioglu, F., and Böke, H. (2015). Sustainable bio-nano composite coatings for the protection of marble surfaces. *J. Cult. Herit.* 16, 299–306. doi: 10.1016/j.culher.2014.07.004

Sacchi, B., Cantisani, E., Giuntoli, G., Salvini, S., Scopetani, C., Rosi, L., et al. (2012). "Bio-polymers as stone protective," in *12th International Congress on Deterioration and Conservation on Stone* (New York, NY), 22–26.

Selwitz, C. (1988). *Cellulose Nitrate in Conservation*. Marina del Key, CA: Getty Conservation Institute.

Song, J. H., Murphy, R. J., Narayan, R., and Davies, G. B. (2009). Biodegradable and compostable alternatives to conventional plastics. *Philos. Trans. R. Soc. Lond. B Biol. Sci.* 364, 2127–2139. doi: 10.1098/rstb.2008.0289

Stloukal, P., Verney, V., Commereuc, S., Rychly, J., Matisova-Rychlá, L., Pis, V., et al. (2012). Assessment of the interrelation between photooxidation and biodegradation of selected polyesters after artificial weathering. *Chemosphere* 88, 1214–1219. doi: 10.1016/j.chemosphere.2012.03.072

Torrisi, A. (2008). Evaluation of five fluorinated compounds as calcarenite protective. *J. Cult. Herit.* 9, 135–145. doi: 10.1016/j.culher.2007.07.006

Tsakalof, A., Manoudis, P., Karapanagiotis, I., Chryssoulakis, I., and Panayiotou, C. (2007). Assessment of synthetic polymeric coatings for the protection and preservation of stone monuments. *J. Cult. Herit.* 8, 69–72. doi: 10.1016/j.culher.2006.06.007

Tsuji, H., Echizen, Y., and Nishimura, Y. (2006). Photodegradation of biodegradable polyesters: a comprehensive study on poly(L-lactide) and poly(3-caprolactone). *Polym. Degrad. Stab.* 91, 1128–1137. doi: 10.1016/j.polymdegradstab.2005.07.007

Vacchiano, C. D., Incarnato, L., Scarfato, P., and Acierno, D. (2008). Conservation of tuff-stone with polymeric resins. *Constr. Build. Mater.* 22, 855–865. doi: 10.1016/j.conbuildmat.2006.12.012

Xing, Q., Ruch, D., Dubois, P., Wu, L., and Wang, W. J. (2017). Biodegradable and high-performance poly(butylene adipate-co-terephthalate)–lignin UV-blocking films. *ACS Sustain. Chem. Eng.* 5, 10342–11035. doi: 10.1021/acssuschemeng.7b02370

Zaidi, L., Kaci, M., Bruzaud, S., Bourmaud, A., and Grohens, Y. (2010). Effect of natural weather on the structure and properties of polylactide/Cloisite 30B nanocomposites. *Polym. Degrad. Stab.* 95, 1751–1758. doi: 10.1016/j.polymdegradstab.2010.05.014

Zimbardo, M., Ercoli, L., Megna, B., and Scaffaro, R. (2019). Collapsibility of metastable sand by non-conventional oedometer tests. *Granul. Matter* 21:1. doi: 10.1007/s10035-018-0854-6